Available online at www.sciencedirect.com
ScienceDirect
Polymer 47 (2006) 8219–8227
polymer
www.elsevier.com/locate/polymer

Molecular dynamics simulation of organic–inorganic copolymers based on methacryl-POSS and methyl methacrylate

Stéphane Bizet, Jocelyne Galy*, Jean-François Gérard

Laboratoire des Matériaux Macromoléculaires/IMP UMR CNRS 5627, Institut National des Sciences Appliquées de Lyon, Bât Jules Verne – 20 Av. Albert Einstein, 69621 Villeurbanne Cedex, France

Received 5 May 2006; received in revised form 13 September 2006; accepted 19 September 2006

Abstract

Atomistic molecular dynamics simulations have been performed to investigate the effects of introducing monofunctional polyhedral oligomeric silsesquioxanes (POSSs) as pendant groups on the polymethyl methacrylate backbone. The effect of POSS loading and of the structure of the organic substituents on the seven silicon atoms, isobutyl groups or cyclohexyl rings, was studied. Calculated volume–temperature behaviour and X-ray scattering profiles were compared with experimental results obtained on copolymers synthesized from POSS and MMA. In the limited time scale used for the simulation, no aggregation can be observed. Cohesive energy density was calculated and found to decrease as POSS was copolymerized with MMA, but in the same order of magnitude whatever the organic ligand nature is. Chain packing around the POSS cluster was evaluated through radial distribution functions. The mobility of the POSS clusters was determined via the mean square displacement. The results tend to confirm the idea that POSS incorporated as dangling groups along the macromolecular backbone behave as anchoring groups.

Keywords: Molecular dynamics; Polymethyl methacrylate; POSS

1. Introduction

For the last decade, hybrid organic–inorganic nanocomposites based on the incorporation of polyhedral oligomeric silsesquioxanes or POSSs™ into polymeric matrices have received a considerable amount of attention. POSS has a compact hybrid structure with an inorganic core made up of silicon and oxygen atoms $(SiO_{1.5})_n$, with $n = 8$, 10, 12, externally surrounded by non-reactive or reactive polymerizable organic ligands [1,2]. The non-reactive ligands, R, are generally isobutyl groups, cyclohexyl or cyclopentyl rings and sometimes phenyl rings. The interactions between the organic ligands and the matrix control the initial solubility of the POSS in the medium, and thus the degree of dispersion of POSS and of property modification. POSS can be dispersed on a molecular level (1–3 nm), or as crystalline or amorphous aggregates, which can be in the order of microns in size. Monofunctional POSS has been incorporated into a variety of conventional polymers, by a variety of polymerization techniques such as radical, condensation, ring-opening polymerization…amongst these polymers polymethyl methacrylate (PMMA) [3–6]. PMMA is a widely used polymer principally due to its high transparency property in visible light. Moreover PMMA is now a matrix of importance in the field of nanocomposite materials [7]. It has been shown in the literature that the chemical nature of the inert organic ligand R plays a major role in the control of the morphologies generated in the hybrid materials, including the possibility to have amorphous or crystalline POSS aggregates; as a consequence the value of the glass transition temperature, T_g, as well as mechanical properties of the copolymers synthesized from POSS and organic monomer depend strongly on the type of POSS considered.

The goal of the present study is to achieve an understanding of the structure–property relationships in atactic poly(MMA-*co*-POSS) using atomistic molecular modelling, especially molecular mechanics (MM) and molecular dynamics (MD)

* Corresponding author. Tel.: +33 4 72 43 83 81; fax: +33 4 72 43 85 27.
E-mail address: jocelyne.galy@insa-lyon.fr (J. Galy).

0032-3861/$ - see front matter © 2006 Elsevier Ltd. All rights reserved.
doi:10.1016/j.polymer.2006.09.040

simulations, in comparison with the experimental data. Molecular dynamics has been shown to be a powerful method of investigation of molecular motion, intra- and intermolecular interactions… This method has been applied successfully to a large range of amorphous thermoplastic polymers, amongst them PMMA [8,9], and clay-based nanocomposites [10–12] but to our knowledge only a few studies deal with POSS-based polymer [13–15]. The strategy chosen falls into two steps: first, to confront experimental and simulated data in terms of X-ray scattering, glass temperature transition…of atactic poly (MMA-*co*-POSS) and secondly to focus on the influence of the structure of POSS on intermolecular interactions and molecular mobility.

2. Experimental

2.1. Material synthesis

(Isobutyl)$_7$Si$_8$O$_{12}$(propyl methacrylate) and (cyclohexyl)$_7$Si$_8$O$_{12}$(propyl methacrylate), denoted *i*BuPOSS and CyPOSS, respectively, were purchased from Hybrid Plastics (Hattiesburg, MS). *i*BuPOSS and CyPOSS are crystalline compounds. The melting temperature for *i*BuPOSS is 109 °C, but no fusion was observed before degradation for CyPOSS. *i*BuPOSS was used as received, but CyPOSS was purified by recrystallization from methanol in order to eliminate residual trisilanol POSS that was evidenced by MALDI-TOF and ^{29}Si NMR spectroscopies as impurity [16]. *i*BuPOSS is easily soluble in solvents such as THF, chloroform, toluene, acetone and also in hexane. The solubility of purified CyPOSS is less, especially in acetone and hexane. Azo-bis-isobutyronitrile free radical initiator (AIBN) and methyl methacrylate (MMA) were purchased from Aldrich and used as received. Chemical structures of monomers are shown in Scheme 1. The copolymer synthesis was done following a protocol described in the literature [3] and is outlined in Scheme 1. In summary, the copolymerization was carried out in a toluene solution for 3 days at 70 °C. 0.25 mol% of AIBN was used. The POSS content was 2.5, 5 and 10 mol% (Table 1). After polymerization the material was precipitated from methanol and purified by two successive precipitations. Then the copolymers were dried at 120 °C under vacuum to achieve total elimination of residual solvents.

2.2. Material characterization

Copolymers composition was determined by both liquid ^{1}H NMR and elemental analysis. Molar mass of the copolymers was determined by size exclusion chromatography (SEC) from Viscotek, using THF as eluant and standard polystyrene calibration. Density was measured by helium picnometry using a Micromeritics Accupyc 1330 apparatus, at room temperature. Wide angle X-ray scattering (WAXS) was carried out on a Siemens D500 apparatus, at room temperature, using the Cu Kα radiation. Thermal analysis (DSC) was performed on a Mettler DSC30 instrument at a heating rate of 10 K/min, under inert atmosphere.

3. Simulation details

3.1. Systems studied

Two series of random copolymers have been studied:

- The first series is based on MMA and isobutyl-POSS with molar fraction of POSS of 2.5, 5 and 10 mol%.
- The second series is based on MMA and cyclohexyl POSS with molar fraction of POSS of 2.5, 5 and 10 mol%.

The hybrid copolymers were built as a single chain with degree of polymerization equal to 80; they are atactic with 50% of meso dyads, a value close to the experimental ones determined using ^{13}C NMR. Depending on the copolymer considered, there were between 1172 and 1666 atoms per chain. The copolymers are compared to a reference polymer, the pure PMMA, built also as a single chain with degree of polymerization equal to 100, with the same tacticity. There were 1502 atoms per chain.

3.2. Molecular dynamics details

All the simulations have been carried out using the Accelrys Amorphous Cell module, employing the COMPASS (condensed phase optimized molecular potentials of atomic simulation studies) force field, both available in Materials Studio software [17]. The COMPASS force field has been used successfully for the simulation of polymer nanocomposites containing POSS [13]. Periodic boundary conditions were used to simulate bulk materials. Temperature and pressure were controlled using the Andersen [18] and Berendsen et al. [19] methods, respectively. The velocity form of the Verlet integrator was used to solve the equations of motion using a time step of 1 fs.

In the energy expression a very important term represents the non-bonded interactions (Van der Waals and electrostatic). However, as this term has a quadratic dependence on the number of atoms in the system it is common to neglect or approximate non-bonded interactions between widely separated pairs of atoms. Choosing how to treat long-range non-bonded interactions is an important factor in determining the accuracy and the time taken to perform an energy calculation. Several cutoff methods can be used. A simple approach is the direct method, called ‘‘atom-based cutoffs’’, where non-bonded interactions are simply calculated on an atom-by-atom basis, to a cutoff distance generally lying between 8 and 10 Å, and interactions beyond this distance are ignored. However, the direct method can lead to discontinuities in the energy and its derivative. To avoid these artifacts cutoffs over charge groups can be used. In this method called ‘‘group-based cutoffs’’, a molecule is considered as a set of small groups which has a net charge of zero. Often charge groups are identical to common chemical functional groups. This method is widely used in polymer simulation; however, its application to our copolymers creates some difficulties due to the size of the POSS molecule. In

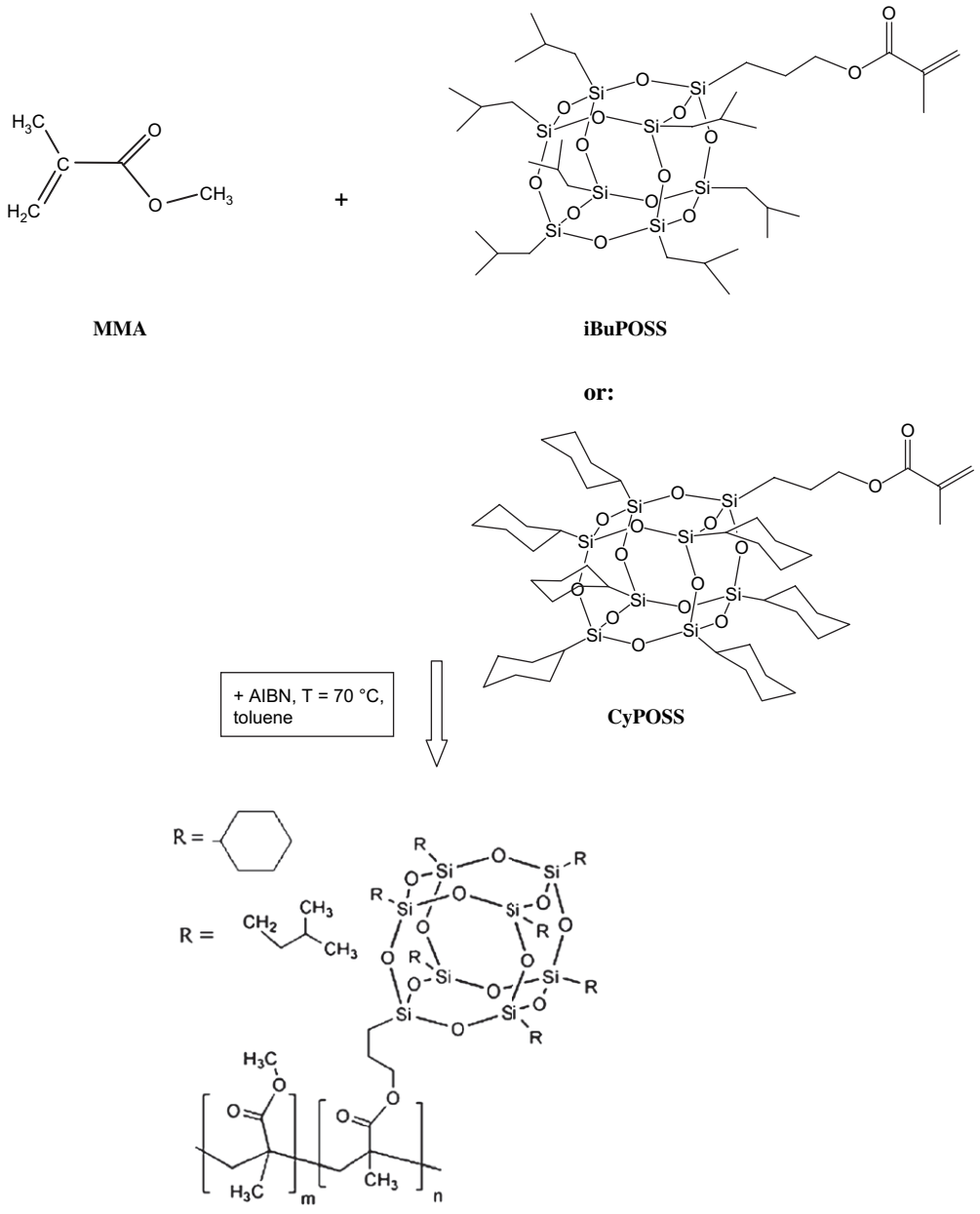

Scheme 1. Chemical structures of monomers and copolymers.

such a ''group-based cutoff'' method the size of the group must be small enough as compared to the cutoff value, typically the group size should not exceed 4/5 Å for a cutoff of 8/10 Å. Following this rule the PMMA chain can be easily decomposed into four neutral groups: CH_3, CH_2, C and O═C−O−CH_3. In the presence of POSS the computing code considers the inorganic cage and the first carbon atoms on the Si corner as a neutral group in a whole. It is due to the fact that the Si/O ratio is not an integer. The size of such a group is higher than the cutoff equal to 9 Å and the method becomes ineffective. Therefore we were obliged to create by ourselves the neutral groups constituting the POSS monomer. The inorganic cage Si_8O_{12} has been decomposed into four neutral groups made of two silicon atoms and three oxygen atoms as shown in Scheme 2. However, in order to have a neutral system we were obliged to adjust the value of the electrostatic charge borne by the oxygen atom in the Si_2O_3 group and also of the carbon atom in the methylene unit in *i*BuPOSS, or in CH in CyPOSS. We will see later in this paper how this decomposition of the copolymer in neutral groups has been validated.

PMMA and the copolymers were built at a low density of 0.7 and 0.3 g cm^{-3}, respectively, to avoid the formation of loops, and subsequently compacted to reach the experimental density, by performing molecular dynamics simulation under NPT (constant particle numbers, pressure and temperature) conditions at 4 GPa and 273 K, followed by a minimisation involving 200 steps. For each kind of polymer 50 independent configurations were initially generated. The configurations with the highest energy were rejected and finally 5−10 configurations were selected for further simulations.

Table 1
Copolymer characteristics

	POSS in feed (mol%)	POSS in copolymer (mol%)	$\overline{M}_n$ (g mol^{-1})	$\overline{D}_{pn}$	Density at 25 °C (g cm^{-3}) ±0.002	T_g (°C) from DSC	T_g (°C) from simulation ±4 °C
PMMA	–	–	41 700	417	1.189	108	178
Poly(MMA-*co*-*i*BuPOSS)	2.5	1.9	48 800	420	1.209	112	–
	5	4.2	50 500	374	1.201	108	187
	10	8.6	66 300	385	1.210	97	167
Poly(MMA-*co*-CyPOSS)	2.5	2.0	43 600	363	1.212	117	–
	5	3.6	45 000	328	1.213	124	188
	10	8.9	57 400	300	1.219	137	199

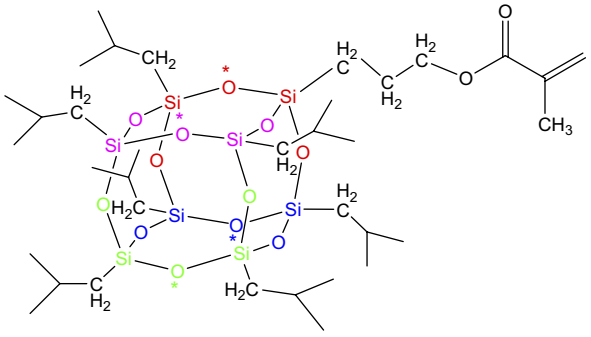

Scheme 2. Decomposition of the POSS cage into neutral groups. *: switching atom.

4. Results and discussion

4.1. Copolymer characterization

The composition, molecular weight, density and glass transition temperature of the copolymers produced are summarized in Table 1. We noted that the mol% of POSS in the final copolymer was systematically less than the mol% in the feed, even if the difference is weak. Such a trend has already been observed [5,20]; this effect is directly related to the reactivity ratio difference: from the data provided by Hybrid Plastics [21], the reactivity ratio for POSS and MMA is 0.584 and 1.607 when R is an isobutyl group, and 0.837 and 1.473 when R is a cyclopentyl group. As a consequence, at the beginning of the polymerization only a few POSSs are incorporated in the macromolecules, while progressively the chain will contain more and more POSS as the polymerization proceeds. The incorporation of POSS leads to a slight increase in the molecular weight of the copolymer; it is due to the high molecular weight of POSS.

All copolymers show a density higher than the density of PMMA. It may be due for one part to the atomic composition, i.e., presence of silicon atoms, but also to the spatial organisation of the polymer chains which is greatly influenced by the presence of POSS. Moreover at the same composition the density of poly(MMA-*co*-*i*BuPOSS) is lower than the one of poly(MMA-*co*-CyPOSS).

There is also a clear influence of the structure of the POSS on the glass transition temperature of the copolymers: when the POSS bears isobutyl groups T_g decreases as compared to pure PMMA; on the contrary if the POSS bears cyclohexyl groups T_g is increased, up to 30 °C when the copolymer has 10 mol% of CyPOSS. A very similar effect has been observed on the T_g of copolymers synthesized from POSS and styrene [22]. Moreover it has been shown that phenyl substituents play the same role as cyclohexyl groups: they contribute to an increase of T_g. The higher the T_g, the stronger the interactions in the copolymers. Modelling studies can help in a number of different ways to understand such behaviour.

4.2. Force field validation – X-ray scattering profiles

At the end of the building protocol described above, the selected configurations were relaxed by an annealing procedure from 1200 K to 300 K, by doing successive NVT dynamics in order to reduce their potential energy. Then during the production step, a configuration was saved every 100 fs during the last 100 ps of the NVT dynamics. The diffractograms of the last configuration were then computed for the two series of copolymers and for PMMA.

The comparison between experimental X-ray scattering intensity profiles and computed ones is shown in Fig. 1. The experimental X-ray pattern of PMMA shows a broad amorphous halo at $2\theta = 14.3°$, it corresponds to a Bragg distance of 6.2 Å, as already reported in the literature [23]. The simulated X-ray profiles of PMMA is in excellent agreement with the experimental results, in terms of peak position and intensity (Fig. 1a).

Upon incorporation of *i*BuPOSS a second amorphous halo at $2\theta = 8.9°$ appears in the experimental patterns of copolymers, and its intensity increases with the amount of *i*BuPOSS (Fig. 1b, c). Such a peak has also been observed on copolymers synthesized from norbornene and POSS [24] or styrene and POSS [25]. This new peak is attributed to the intermolecular organisation of the POSS molecule. From the shape of the peak it is clear that the copolymers from MMA and *i*BuPOSS are all amorphous. This result was confirmed by transmission electron microscopy (TEM) which revealed that the copolymers were homogeneous without any aggregates [26]. Moreover for high content of *i*BuPOSS we observed a shift of the first amorphous halo at $2\theta = 14°$ to higher diffraction angles coupled with a strong decrease in intensity. It indicates that the organisation of the chains in the copolymer becomes different from the one of pure PMMA. The predicted scattering

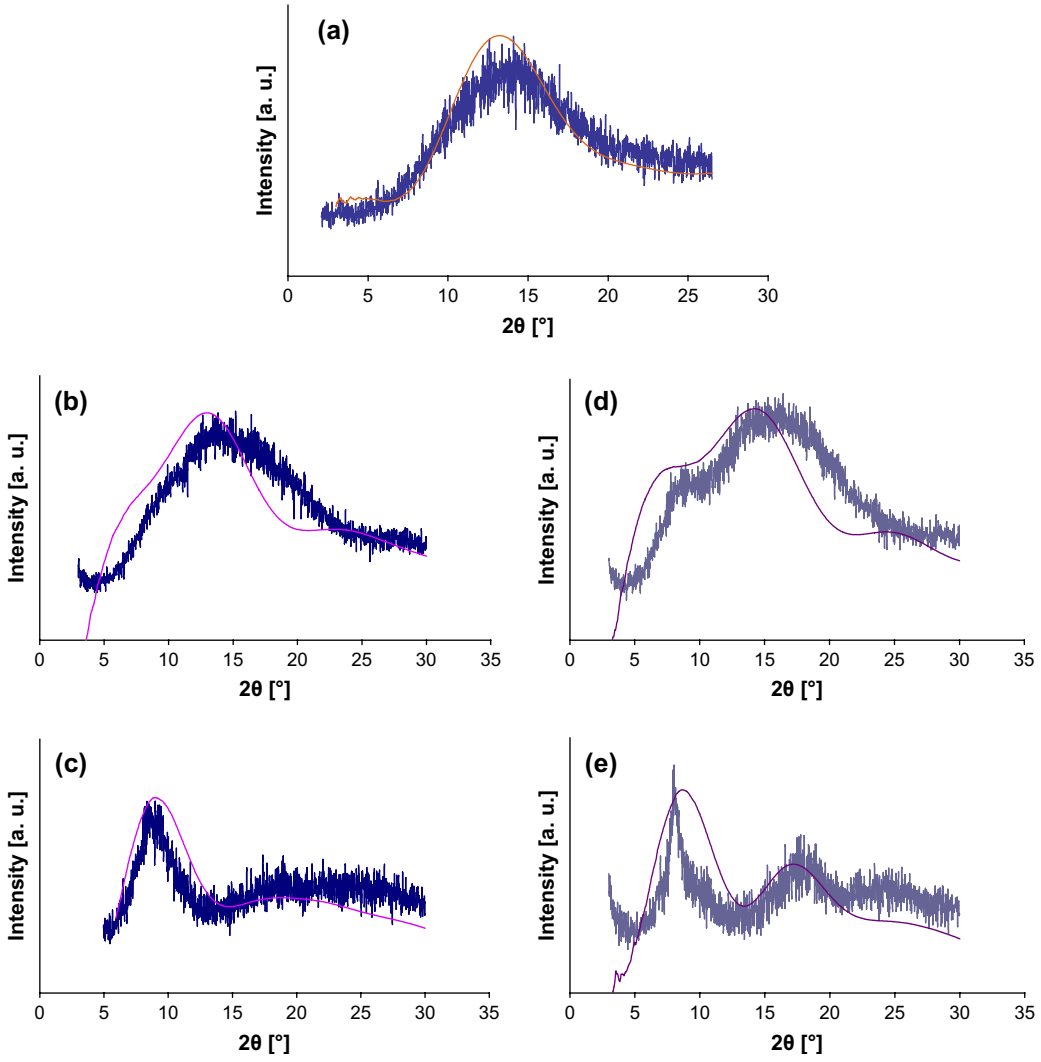

Fig. 1. Computed (thin line) and experimental WAXS patterns (arbitrary units): (a) PMMA; (b) poly(MMA-*co*-2.5 mol% *i*BuPOSS); (c) poly(MMA-*co*-10 mol% *i*BuPOSS); (d) poly(MMA-*co*-2.5 mol% CyPOSS); (e) poly(MMA-*co*-10 mol% CyPOSS).

profiles obtained from molecular modelling, for the copolymer built with 2.5 and 10 mol% of *i*BuPOSS (Fig. 1b, c) show a very good agreement with the experimental profiles: peak positions are identical as well as respective intensity.

The same trends are observed on the experimental patterns when CyPOSS is used to synthesize the copolymers: appearance of a peak at $2\theta = 8^\circ$ ($d = 11$ Å), with an increase in the intensity with increasing amounts of CyPOSS. However, the intensity and the shape of this peak indicate a strong tendency of CyPOSS towards association, contrary to *i*BuPOSS. Especially for the copolymer synthesized with 10 mol% of CyPOSS, the thinness of this peak is the proof of the crystalline organisation of CyPOSS in the medium. This result is not so surprising because such observations were already noticed in the literature [24,25]. So from the experimental diffractogram it can be concluded that this copolymer has a heterogeneous structure. Moreover TEM micrographs confirmed the WAXS experiments: the copolymer synthesized with 2.5 mol% is homogeneous while the copolymers synthesized with 5 and 10 mol% of CyPOSS exhibit a lamellar-like morphology, with a random orientation of the platelets [26]. The simulated diffractogram of the copolymer built with 2.5 mol% of CyPOSS is in very good agreement with the experimental one (Fig. 1d) because of the homogeneous and amorphous nature of this material. As the amount of POSS reaches 10 mol% some interesting features appear: the simulated diffractograms are close to the experimental one if we look at the peak position and the peak intensity; however, the shape of the simulated peak at $2\theta = 8^\circ$ does not fit the experimental one. This result is perfectly normal if we remember that the synthesized copolymer shows a crystalline lamellar organisation. Such an organisation is impossible to reach in the simulated copolymer, because of the very short time scale of molecular dynamics, most of the time less than 1 ns, as compared to the time scale of crystallization or aggregation phenomena. Simulations of at least 10 ns associated to powerful parallelized machines are needed to observe particle aggregation [14]. As a consequence of this well-known drawback of molecular modelling, our simulated copolymers are always amorphous. In the real copolymers, it is effectively the case

for the materials based on *i*BuPOSS and 2.5 mol% of CyPOSS, but it is no more true for the materials synthesized with at least 5 mol% of CyPOSS which show some crystalline domains. In this latter case, the diffractograms and further simulations we obtained after running the dynamics can be seen as representative only of the amorphous part of the material, in which the CyPOSS is individually and randomly dispersed.

Considering the excellent agreement we reached between simulated and experimental X-ray profiles on PMMA and on poly(MMA-*co*-*i*BuPOSS), we can conclude that the COMPASS force field, and also our building and simulation protocols, particularly the charge group attribution, allow us to generate polymers with intra- and intermolecular organisation representative of real systems. This result is of interest if we have in mind the difference between the real and simulated copolymers: chain length, polydispersity, chain architecture… So the comparison of X-ray profiles is a very good criterion for the selection of the best configurations for further simulations.

4.3. Volume–temperature behaviour

The computation of the volume–temperature (V–T) diagram using molecular dynamics allows the prediction of the glass transition temperature, in spite of the time scale considered [27]. In simulation, the specific volumes are predicted as a function of temperature at a given pressure via NPT dynamics. The simulation protocol was run on well-equilibrated samples, which were cooled down from 650 K, in 25 K intervals, undergoing NPT dynamics at each isothermal temperature for 100 ps. The V–T diagram for each polymer has been obtained by averaging the value of specific volume at each T, over 10 different configurations. Fig. 2 shows the plot of specific volume vs. temperature for the pure PMMA and the copolymers built with 5 and 10 mol% of POSS. In all cases, the diagrams show similar trends: the temperature at which a break in slope occurs designates the glass transition temperature. The fact that T_g can be clearly observed means that the size of the systems is large enough as compared to the characteristic length of the domains involved in the glass transition phenomenon. The glass transition temperatures from simulations are systematically higher than the experimental ones. This fact has already been reported in the literature [8] and is explained mainly by the difference in the cooling rate in simulation ($\sim 10^{11}$ K/s) and in the DSC oven (10 K/min). Longer trajectories of a few ns would be required to reduce the difference between simulated and experimental values. The most important observation is that the incorporation of CyPOSS into the PMMA backbone increases the T_g, while the incorporation of *i*BuPOSS decreases the T_g. Both observations are in agreement with experimental results (Table 1). This result is an additional proof of the accuracy of the force field and protocols used. However, we can note that the increase in the simulated T_g, ΔT_g, of the copolymers based on CyPOSS, as compared to pure PMMA, is lower than the experimental one. This is due to the difference in structure of the copolymers: the simulated ones are completely amorphous while the real ones exhibit a crystalline organisation. In these semi-crystalline copolymers,

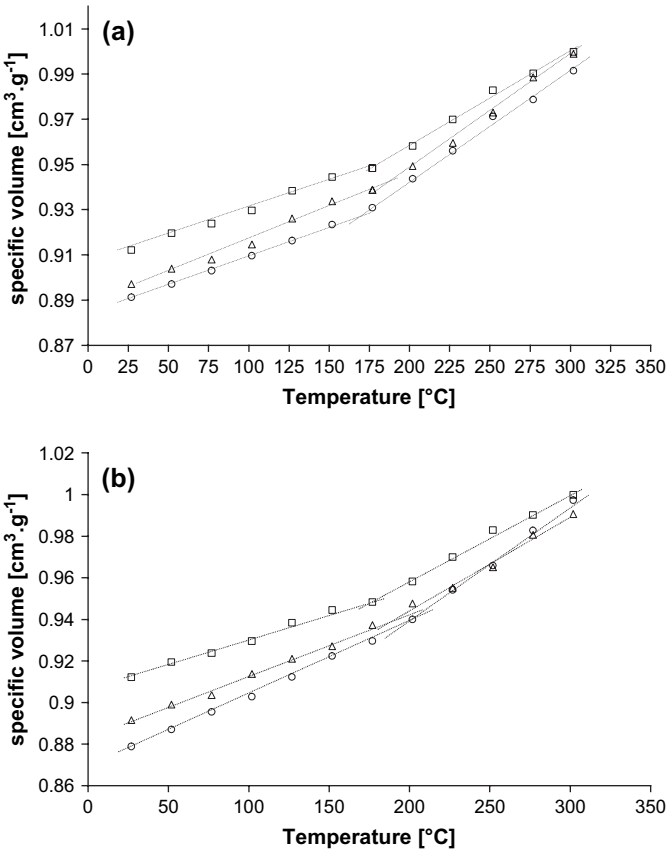

Fig. 2. Specific volume vs. temperature for: PMMA: (□); poly(MMA-*co*-5 mol% POSS): (△); poly(MMA-*co*-10 mol% POSS): (○). (a) *i*BuPOSS; (b) CyPOSS.

the increase of T_g is attributed one part to the CyPOSS homogeneously dispersed on the material and another part to the presence of the crystalline lamellas, which restrict the molecular motions of the surrounding chains.

4.4. Cohesive energy

The cohesion of a polymer material results from attractive intermolecular interactions, mainly Van der Waals and hydrogen bonding interactions, and to a less extent Coulombic interactions. The cohesive energy represents the sum of the energy of all the intermolecular interactions. Normalization of the cohesive energy with molar volume, V_m, yields the cohesive energy density, CED. The solubility parameter, δ, is simply the square root of the cohesive energy density. It is a parameter of great importance in the field of the thermodynamics of polymer blends and it is not trivial to determine it experimentally with good accuracy. No data are available for δ, on poly(MMA-*co*-POSS). In atomistic simulation, the cohesive energy represents the increase of potential energy when all the intermolecular interactions are suppressed. In concrete terms, the potential energy of a 3D periodic cell is calculated, E_{3D}, taking into account tail corrections, ΔU_{tail}. These corrections are needed to take into consideration the error introduced by the cutoff method. Then the periodic boundary conditions

are removed, i.e., intermolecular interactions are removed, and the potential energy of the single macromolecule is calculated, E_s. The solubility parameter is obtained by:

$$\delta = \sqrt{\frac{E_s - (E_{3D} + \Delta U_{tail})}{V_m}}$$

The simulations were done on well-equilibrated 3D structures by running NVT dynamics at 300 K. The simulation was repeated on 10 different configurations for each polymer, and the solubility parameter given is the average value. Solubility parameters are shown in Fig. 3 for the two series of polymers. The values obtained for the copolymers are lower than the value obtained on pure PMMA, $\delta = 16.4\ \mathrm{MPa}^{1/2}$. Moreover, a clear decrease of δ is observed as the amount of POSS is increased: δ reaches a value around $14\ \mathrm{MPa}^{1/2}$ as 10 mol% of POSS is copolymerized with MMA. It means that the intermolecular interactions in the poly(MMA-*co*-POSS) are reduced as compared to PMMA, despite the fact that the copolymers are more dense. For a given molar fraction of POSS, the values of δ are identical for CyPOSS or *i*BuPOSS. There is no influence of the structure of the organic ligand, cyclohexyl or isobutyl. It is not really surprising because their structure is very similar so they develop similar intermolecular interactions. Similar conclusions have been reported by Bharadwaj et al. [13], i.e., a decrease of 3–4 $\mathrm{MPa}^{1/2}$ of the solubility parameter of polynorbornene when POSS is copolymerized with norbornene. The solubility parameter can be considered according to two terms: the electrostatic contribution and the Van der Waals contribution. In PMMA, the main contribution to δ is the Van der Waals contribution even if there is also a weak contribution to the electrostatic term due to the polar carbonyl groups. In the presence of POSS the decrease of the intermolecular interactions results from the decrease of both types of interactions [16]. This decrease of the Van der Waals intermolecular interactions is a little striking because one could expect to introduce Van der Waals interactions by replacing a methyl methacrylate monomer by a POSS monomer, this increase being a consequence of the increase of the total number of atoms. So, to have a better understanding of this effect, molecular packing was investigated for all copolymers and PMMA.

4.5. Influence of POSS on macromolecular organisation

The packing details of the different polymers can be estimated through pair correlation function, also referred to as radial distribution function, $g(r)$. $g(r)$ is defined as the probability of finding a pair of atoms (α, β) that are separated by a radial distance $r_{\alpha\beta}$, relative to the probability that is expected for a completely random distribution. So it yields information about the average interchain spacing of the polymer. Fig. 4 shows the intermolecular pair correlation function based on all the atoms of the chain, for the different polymers. No diffuse peak, significant of an average interchain packing, can be seen. So from our simulation it is not possible to conclude that POSS has a clear influence on the average distance between neighboring chains. However, the $g(r)$ behaviour is different for the five polymers. Between 2 and 10 Å, the radial distribution function is the highest for PMMA. It means that, at any given distance, the number of "contacts" between neighboring chains is decreased due to the presence of POSS. Moreover this number decreases with increasing molar fraction of POSS. So finally, we can conclude that the decrease of the intermolecular interactions results mainly from the decrease of the number of interactions rather than from a distancing of the chains. The reduction in the number of intermolecular contacts can be explained by the large size of the cluster. These clusters induce a large excluded volume to the detriment of interchain contacts. Similar conclusions are reported in the literature [13,28]. In addition, the intermolecular pair correlation function based on all the atoms (Si, O) from the POSS in the copolymers to the atoms in the main chains is shown in Fig. 5. For a same molar content of POSS, i.e., 5 or 10 mol%, the $g(r)$ has a higher value at any given r, for poly(MMA-*co*-*i*BuPOSS) compared to poly(MMA-*co*-CyPOSS). It indicates that the number of contacts between POSS and neighboring chains is higher in the case of isobutyl-POSS. So there is a clear difference of organisation around

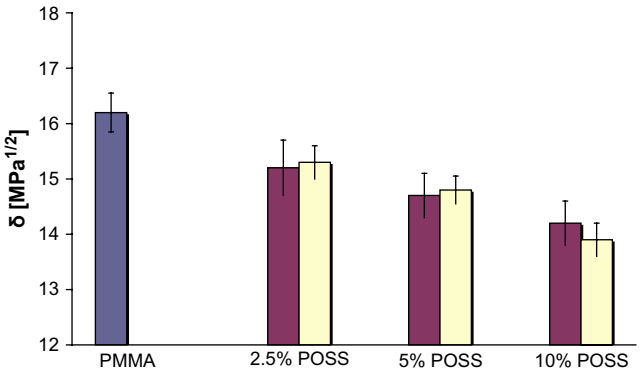

Fig. 3. Solubility parameters, δ, for: PMMA: (■), poly(MMA-*co*-*i*BuPOSS): (■); poly(MMA-*co*-CyPOSS): (■). (For interpretation of the references to color in this figure legend, the reader is referred to the web version of this article.)

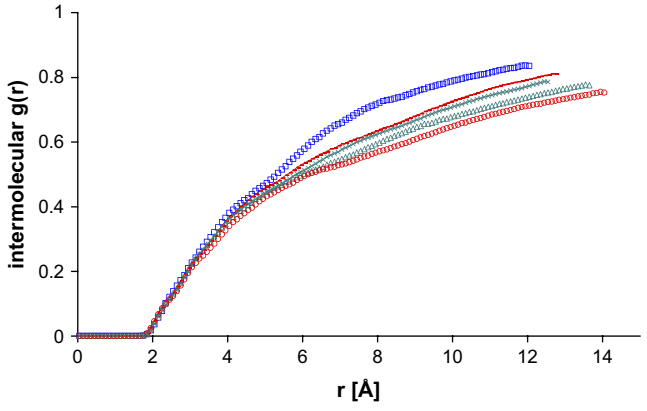

Fig. 4. Pair correlation functions, $g(r)$, based on all backbone atoms for: PMMA: (□); poly(MMA-*co*-5 mol% *i*BuPOSS): (×); poly(MMA-*co*-5 mol% CyPOSS): (-); poly(MMA-*co*-10 mol% *i*BuPOSS): (△); poly(MMA-*co*-10 mol% CyPOSS): (○).

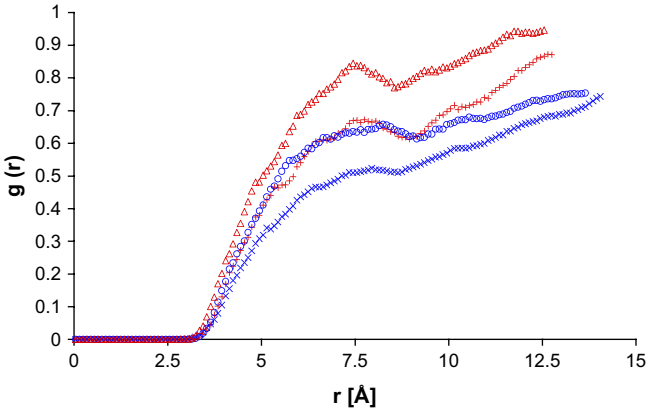

Fig. 5. Pair correlation functions, $g(r)$, based on all POSS atoms, to the atoms in the main neighboring chain: poly(MMA-*co*-5 mol% *i*BuPOSS): (△); poly(MMA-*co*-5 mol% CyPOSS): (+); poly(MMA-*co*-10 mol% *i*BuPOSS): (○); poly(MMA-*co*-10 mol% CyPOSS): (×).

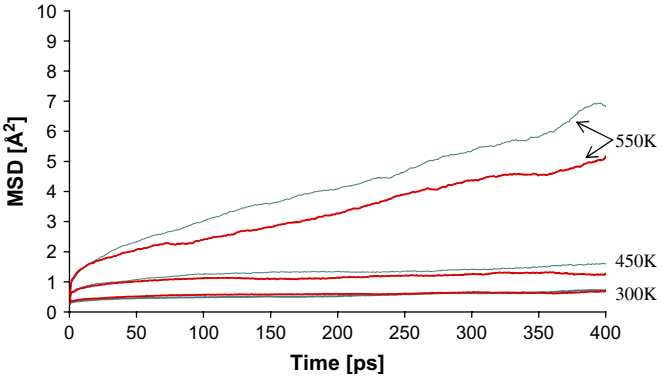

Fig. 7. Mean square displacement of the silicon and oxygen atoms in POSS core (—) in poly(MMA-*co*-10 mol% *i*BuPOSS) and in poly(MMA-*co*-10 mol% CyPOSS) (—), at different temperatures. (For interpretation of the references to color in this figure legend, the reader is referred to the web version of this article.)

the cluster, depending on the structure of the organic ligand. Isobutyl groups are more flexible and less bulky than cyclohexyl groups; therefore the packing of the chains around the cluster is easier.

4.6. Influence of POSS on molecular dynamics

The intrinsic mobility of the POSS clusters can be estimated through the mean square displacement (MSD) of the silicon and oxygen atoms of the POSS core. The MSD was computed from the following expression:

$$\mathrm{MSD}(\Delta t) = \left\langle |r_i(t_0 + \Delta t) - r_i(t_0)|^2 \right\rangle$$

where $r_i(t)$ represents the coordinates of atom i, at time t. The average of the MSD is taken along the original simulation trajectory, over all the atoms of type i.

Fig. 6 compares the mean square displacement of all atoms in the poly(MMA-*co*-10 mol% *i*BuPOSS) to the MSD of the oxygen and silicon atoms of the *i*BuPOSS cluster, at different temperatures. Whatever the temperature, 400 K or 550 K, the mean square displacement of POSS is 3–4 times smaller than that of the macromolecule as a whole. This result confirms the idea that the monofunctional POSS acts as an anchoring point to which the macromolecule is linked. Fig. 7 shows the influence of the organic ligand, on the MSD of the atoms of the POSS core at different temperatures. Up to 450 K the behaviour is non-diffusive and the POSS looks stationary: the MSD is found to be close to 1 Å for both types of POSS. At 550 K, we observe the onset of diffusive behaviour. However, even at this temperature, the magnitude of the MSD is low. The very low mobility of the silsesquioxane polyhedra, as pendant objects in a macromolecular chain, is confirmed. We also noticed that the *i*BuPOSS leads to a slightly higher MSD, compared to CyPOSS, at 550 K. This result is in agreement with the higher glass transition temperature obtained on poly(MMA-*co*-CyPOSS) as compared to poly(MMA-*co*-*i*BuPOSS).

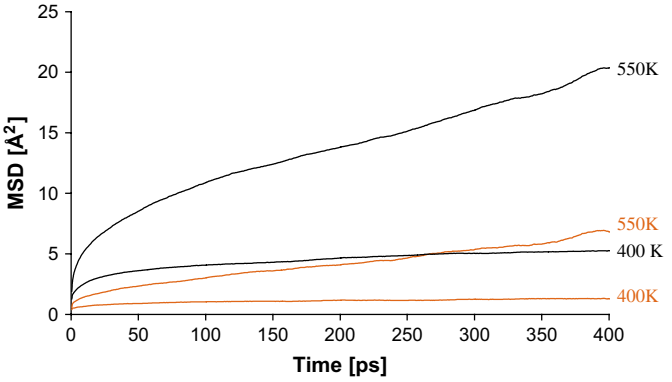

Fig. 6. Mean square displacement at 400 K and 550 K of: all atoms (—), silicon and oxygen atoms in *i*BuPOSS core (—) in poly(MMA-*co*-10 mol% *i*BuPOSS). (For interpretation of the references to color in this figure legend, the reader is referred to the web version of this article.)

5. Conclusions

The objectives of this molecular modelling study was to investigate the influence of POSS introduced as pendant groups onto PMMA chains, on the intermolecular interactions and on the mobility at a molecular level. Despite some unavoidable differences between experimental and simulated systems, in particular concerning the morphologies generated, the following conclusions can be drawn:

(i) A very good agreement between simulated predicted X-ray scattering intensities and experimental ones proved the accuracy of the force field and simulation protocols used.

(ii) An increase of the glass transition temperature was predicted by the simulation when CyPOSS is copolymerized with MMA while a decrease of T_g was predicted when *i*BuPOSS is used instead of CyPOSS. Both observations are in full agreement with the experimental data.

(iii) The calculation of the cohesive energy density shows that the incorporation of these POSS nano-objects reduces the intensity of the intermolecular interactions between neighboring macromolecules, mainly because of the large volume fraction occupied by the POSS and of their non-polar character.

(iv) The mobility of the POSS was evaluated via the mean square displacement; POSS has a very low mobility and therefore can be viewed as anchoring points linked to the macromolecules. However, the effect of POSS on molecular mobility is not restricted to an inertia effect, it is much more complex. The strong influence of the chemical structure of the organic ligands on the molecular motion suggests that other factors like the intrinsic mobility of the ligands and the organisation of the chains around the POSS clusters play a role.

Acknowledgments

This work was supported by the French Ministry of Education and by the European Community through Research Training Network funded under the 5th framework programme, under contract HPRN-CT-2002-00306 ‘‘NBB-HYBRIDS’’.

References

[1] Provatas A, Matisons JG. Trends Polym Sci 1997;5:327.
[2] Li GZ, Wang LC, Ni HL, Pittman CU. J Inorg Organomet Polym 2001; 11:123.
[3] Lichtenham JD, Otanari YA, Carr MJ. Macromolecules 1995;28:8435.
[4] Kopesky ET, Haddad TS, Cohen RE, McKinley GH. Macromolecules 2004;37:8992.
[5] Xiao J, Feher FJ. Polym Prepr 2002;43:504.
[6] Zhang W, Fu BX, Schrag E, Hsiao B, Mather PT, Yang N, et al. Macromolecules 2002;35:8029.
[7] Ash BJ, Siegel RW, Schadler LS. Macromolecules 2004;37:1358.
[8] Soldera A, Grohens Y. Macromolecules 2002;35:722.
[9] Soldera A, Metale N. Composites Part A Appl Sci Manuf 2004.
[10] Pospisil M, Capkova P, Weiss Z, Malac Z, Simonik J. J Colloid Interface Sci 2002;245:126.
[11] Toth R, Coslanich A, Ferrone M, Fermiglia M, Pricl S, Miertus S, et al. Polymer 2004;45:8075.
[12] Zheng QH, Yu AB, Lu GQ, Standish RK. Chem Mater 2003;15: 4732.
[13] Bharadwaj RK, Berry RJ, Farmer BL. Polymer 2000;41:7209.
[14] Capaldi FM, Rutledge GC, Boyce MC. Macromolecules 2005;38: 6709.
[15] Chan ER, Zhang X, Lee CY, Neurock M, Glotzer C. Macromolecules 2005;38:6168.
[16] Bizet S. PhD thesis, 04 ISAL 0099; 2004.
[17] <http://www.accelrys.com>.
[18] Andersen HC. J Chem Phys 1980;72:2384.
[19] Berendsen HJC, Potsma JPM, van Gunsteren WF, DiNola A, Haak JR. J Chem Phys 1984;81:3684.
[20] Haddad TS, Lichtenhan JD. Macromolecules 1996;29:7302.
[21] <http://www.hybridplastics.com>.
[22] Haddad TS, Viers BD, Phillips SH. J Inorg Organomet Polym 2002; 11:155.
[23] Miller RL, Boyer RF. J Polym Sci Part B Polym Phys 1984;22:2021.
[24] Mather PT, Jeon HG, Romo-Uribe A, Haddad TS, Lichtenhan JD. Macromolecules 1999;32:1194.
[25] Romo-Uribe A, Mather PT, Haddad TS, Lichtenhan JD. J Polym Sci Part B Polym Phys 1998;36:1857.
[26] Amici M. PhD thesis, 06 ISAL 004; 2006.
[27] Han JC, Gee RH, Boyd RH. Macromolecules 1994;27:7781.
[28] Xu H, Kou S-W, Lee JS. Macromolecules 2002;35:8788.